ISSN NO. 2320-5407

Journal homepage: http://www.journalijar.com

INTERNATIONAL JOURNAL OF ADVANCED RESEARCH

RESEARCH ARTICLE

Whistler Mode Wave by Cold Plasma Injection for Relativistic Generalized Loss-Cone Distribution Function in the Magnetosphere of Uranus

R.S. Pandey, Rajbir Kaur and U.C. Srivastava
Department of Applied Physics, Amity Institute of Applied Sciences, Amity University, Noida, U.P. India.

Manuscript Info

Manuscript History:

Received: 12 August 2013
Final Accepted: 20 August 2013
Published Online: September 2013

Key words:
Whistler mode waves,
Cold plasma injection,
Magnetosphere of Uranus

Abstract

In present paper the effect of cold electron beam on field aligned whistler mode wave in the presence of perpendicular AC field in background plasma having relativistic bi-Maxwellian distribution function in the magnetosphere of Uranus was analyzed. Also relativistic and non-relativistic loss-cone distribution function had been examined separately. In all the three cases the effect of cold plasma injection and other plasma parameters had been derived by using characteristic solution and discussed. It was found that growth rate increases by increasing the value of AC frequency for Maxwellian and Loss-Cone background. The effect of ratio of cold injected electron plasma to background plasma density (n_c/n_w) increases the growth rate. In these cases, when such a situation as mentioned, exists in the magnetosphere, it gives rise to emissions over a broad frequency range and would be more suitable for explaining the entire frequency spectrum of VLF emissions.

Introduction

The plasma wave spectrum at Uranus is dominated largely by whistler mode emissions (Gurnett et al. 1986). Whistlers are low frequency, circularly polarized electromagnetic waves in the audio-frequency range. Wave particle interaction can also create whistler mode radiations in the magnetosphere. Whistler mode waves propagating in the magnetosphere of Uranus provide a variety of interesting effects. Whistler waves are also important for the survey of wave phenomena. For the detailed study of such mode of waves, it can be assumed that plasma consist of two species of electron; hot and cold electrons. In addition to high frequency radio emission, whistler mode radiations, which occurred both as a steady hiss and at closest approach in the form of rising chorus, were also identified by Voyager-2. Many familiar plasma waves during exploration of magnetospheres of Earth, Jupiter, Saturn, Uranus and Neptune were observed by several space plasma wave instruments (Gurnett et al. 1979a; Gurnett et al. 1979b; Gurnett et al. 1996; Gurnett et al. 2005; Gurnett et al. 1989; Gurnett et al. 1988; Scarf et al. 1979; Kurth et al. 1980; Kurth et al. 1983; Kurth et al. 1987; Kurth et al. 1991; Zarka et al. 2004).

Whistlers can be generated in quiescent plasma owing to many types of instabilities. One such example is instability produced due to beam of electrons. Such mechanism leading to generation of artificially triggered emissions (ATEs) result from resonant interactions of energetic electrons in the Uranian magnetosphere. The resonant interaction between particles and plasma waves often occur for velocities well above the thermal speed. It is known that resonant wave-particle interaction is the main source of pitch-angle and energy diffusion of trapped electrons in the radiation belt (Kennel et al. 1966).
Electromagnetic and electrostatic instabilities driven by loss-cone distribution explain a variety of plasma phenomena. Summers and Thorne (1995) found that, for parallel propagation, electromagnetic instabilities are only affected by the loss-cone indices in terms of their occurrence in the temperature anisotropy. Also, the thermal anisotropy is caused by the loss-cone property of open-ended magnetic field that posses particles with different velocity classes. This anisotropy can lead to instabilities which transfer plasma kinetic energy into wave energy (Kennel et al. 1966). In general, for small values of pitch angle, loss-cone distribution has deficiency of particles. This distribution typically arises when plasma is confined in a magnetic trap. It was inferred that the

source of free energy for wave excitation can be provided either by a loss-cone feature or by the temperature anisotropy of energetic particles (Denton et al. 1992). Summers et al. (1995) and Huang et al. (1990) had explained various phenomena occurring in plasma, including particle losses, harmonic emissions and specific mode of wave propagation, using both electrostatic and electromagnetic instabilities associated with loss-cone distribution.

Plasma parameters and energetic particle characteristic distributions, through most of the Uranian magnetosphere, are also deeply studied with the help of whistler mode waves. A substantial increase in the energetic electron precipitation was found by the injection of very modest amount of cold plasma into the radiation belt of magnetosphere (Brice et al. 1971). Since then, because of the possibility of excitation of specific modes in magnetosphere, more investigations have been done in whistler mode instability. Misra and Singh (1980) analyzed whistler mode instability by cold plasma injection considering presence of parallel DC electric field (Ganguli et al. 1984) focused on temporal evolution of whistler growth in a time dependent cold plasma injection experiment. It concluded that cold lithium injection in the AMPTE parameter range can lead to whistler mode turbulence. In the inhomogeneous magnetosphere of Uranus, modifications in the oblique whistler mode produced by cold plasma injection in the background, bi-Maxwellian or loss-cone drifted plasma in the presence of perpendicular AC electric field was studied by Pandey et al. (2002). They concluded that magnitude of AC electric field has almost no effect on growth rate but AC frequency affects it. Also the effect of cold plasma injection on whistler mode instability was studied by describing cold plasma applying a simple Maxwellian distribution whereas a generalized distribution function with index j, which reduces to bi-Maxwellian for j=0 and to loss-cone for j=1, to form a hot/warm background (Pandey et al. 2003). One of the significant results drawn from it was that loss-cone background plasma had a triggering effect on the growth rate, increasing the value of the real frequency and maximum growth rate by an order of magnitude.

Motivated by above research, the effect of cold electron beam on field aligned whistler mode wave in the presence of perpendicular AC field in the magnetosphere of Uranus is analyzed in present paper. Background plasma having relativistic bi-Maxwellian, relativistic loss-cone and non-relativistic loss-cone distribution functions have been examined separately. In all the three cases the effect of cold plasma injection and other plasma parameters have been derived by using characteristic solution and discussed.

Dispersion Relation and Growth Rate

A homogeneous anisotropic collision less plasma in the presence of an external magnetic field $B_0 = (B_0 e_z)$ and an electric field $E_{ox} = E_o \sin\upsilon t\, e_x$ is assumed. In interaction zone inhomogeneity is assumed to be small. In order to obtain the particle trajectories, perturbed distribution function and dispersion relation, the linearised Vlasov-Maxwell equations are used. Separating the equilibrium and non equilibrium parts, neglecting the higher order terms and following the techniques of Pandey et. a1 (2003) the linearized Vlasov equations are given as:

$$v.\left(\frac{\delta f_0}{\delta r}\right)+\left(\frac{e_s}{m_e}\right)\left[E_0\sin\upsilon t+\frac{(v\times B_0)}{c}\right].\left(\frac{\delta f_0}{\delta r}\right)=0 \qquad ...(1)$$

$$\left(\frac{\delta f_1}{\delta r}\right)+v.\left(\frac{\delta f_1}{\delta r}\right)+\left(\frac{F}{M_e}\right).\left(\frac{\delta f_1}{\delta r}\right)=S(r,v,t) \qquad ...(2)$$

Where the force

$$F=e\left[E_0\sin\upsilon t+\frac{(v\times B_0)}{c}\right]=m\frac{dv}{dt} \qquad ...(3)$$

Where υ is AC frequency and the dispersion relation is defined as

$$S(r,\mathrm{v},t,) = -\left(\frac{e_s}{m_e}\right)\left[E_1 + \frac{(\mathrm{v}\times B_0)}{c}\right].\left(\frac{\delta f_1}{\delta r}\right) \qquad ...(4)$$

where s denotes the type of electrons. Subscript '0' denotes the equilibrium values. The perturbed distribution function f_1 is determined by using the method of characteristic, which is

$$f_1(r,\mathrm{v},t) = \int_0^{\infty} S\{r_0(r,\mathrm{v},t,),\mathrm{v}_0(r,\mathrm{v},t)),t-t'\}dt$$

we have transformed the phase space coordinate system for (r, v, t) to (r_0, v_0 t - t'). The relativistic particle trajectories that have been obtained by solving equation (3) for given external field configuration are

$$X_0 = X + \left(\frac{P_\perp \sin\theta}{\omega_c m_c}\right) - \left[P_\perp \sin\left\{\frac{\theta + \left(\frac{\omega_c t}{\beta}\right)}{\omega_c m_c}\right\}\right] + \left[\frac{\Gamma_x \sin \upsilon t}{\beta\left\{\left(\frac{\omega_c}{\beta}\right)^2 - \upsilon^2\right\}}\right] - \left[\frac{\upsilon\Gamma_x \sin\left(\frac{\omega_c t}{\beta}\right)}{\omega_c\left\{\left(\frac{\omega_c t}{\beta}\right) - \upsilon^2\right\}}\right]$$

$$Y_0 = Y - \left(\frac{P_\perp \cos\theta}{\omega_c m_c}\right) - \left[P_\perp \cos\left\{\frac{\theta + \left(\frac{\omega_c t}{\beta}\right)}{\omega_c m_c}\right\}\right] + \left(\frac{\Gamma_x}{\upsilon\omega_c}\right) - \frac{\left\{1 + \upsilon^2\beta^2 \cos\left(\frac{\omega_c t}{\beta}\right) - \omega_c^2 \cos\upsilon t\right\}}{\beta^2\left\{\left(\frac{\omega_c}{\beta}\right)^2 - \upsilon^2\right\}}$$

$$z_0 = z - \frac{P_z}{\beta m_e} \qquad ...(5)$$

and the velocities are

$$\mathrm{v}_{xo} = P_\perp \cos\left\{\theta + \frac{\left(\frac{\omega_c t}{\beta}\right)}{\beta m_e}\right\} + \left[\frac{\upsilon\Gamma_x}{p\left\{\left(\frac{\omega_c}{\beta}\right)^2 - \upsilon^2\right\}}\right]\left\{\cos\upsilon t - \cos\left(\frac{\omega_c t}{\beta}\right)\right\}$$

$$v_{yo} = P_\perp \sin\left\{\theta + \frac{\left(\frac{\omega_c t}{\beta}\right)}{\beta m_e}\right\} + \left[\frac{\Gamma_x}{\beta\left\{\left(\frac{\omega_c}{\beta}\right)^2 - \upsilon^2\right\}}\right]\left\{\left(\frac{\omega_c}{\beta}\right)\sin\upsilon t - \upsilon\sin\left(\frac{\omega_c t}{\beta}\right)\right\}$$

$$v_{zo} = \frac{P_z}{\beta m_e} \qquad ...(6)$$

$$v_x = \frac{P_\perp \cos\theta}{\beta m_e}, \qquad v_y = \frac{P_\perp \sin\theta}{\beta m_e}, \qquad v_z = \frac{P_z}{\beta m_e}$$

$$\Gamma_x = \frac{eE_o}{m_e}, \qquad m_e = \frac{m_s}{\beta}, \qquad \beta = \sqrt{1-\frac{v^2}{c^2}}, \qquad \omega_c = \frac{eB_0}{m_e}$$

$P_\perp$ and P_z denote momenta perpendicular and parallel to the magnetic field. Using equation (6), (7) and the Bessel identity and performing the time integration, following the technique and method of Misra and Pandey (1995), the perturbed distribution function is found after some lengthy algebraic simplifications as :

$$f_1 = -\left(\frac{ie_s}{me\beta\omega}\right)\sum J_s(\lambda_3)\exp i(m-n)\theta\left[\frac{J_m J_n J_p U^* E_{1x} - iJmV^* E_1 + J_m J_n J_p W^*}{\omega - \left(\frac{k_\parallel P_z}{\beta m_e} + p\upsilon - \frac{(n+g)\omega_c}{\beta}\right)}\right] \qquad ...(7)$$

Due to the phase factor the solution is possible when m = n. Here.

$$U^* = \left(\frac{c_1 P_\perp n}{\beta\lambda_1 m_e}\right) - \left(\frac{n\upsilon c_1 D}{\lambda_1}\right) + \left(\frac{p\upsilon c_1 D}{\lambda_2}\right)$$

$$V^* = \left(\frac{c_1 P_\perp J_n J_p}{\beta\lambda_1 m_e}\right) + c_1 D J_p J_n \omega_c$$

$$W^* = \left(\frac{n\omega_c F m_e}{k_\perp P_\perp}\right) + \left(\frac{\beta m_e P_\perp \omega \partial f_0}{\partial P_z}\right) + G\left\{\left(\frac{p}{\lambda_2}\right) - \left(\frac{n}{\lambda_1}\right)\right\}$$

$$C_1 = \left\{\frac{(\beta m_e)}{P_\perp}\right\}\left(\frac{\partial f_0}{\partial P_\perp}\right)\left(\omega - \frac{k_\parallel p_z}{\beta m_e}\right) + k_\parallel \beta m_e \left(\frac{\partial f_0}{\partial P_\perp}\right)$$

$$D = \left[\frac{\Gamma_x}{\beta\left\{\left(\frac{\omega_c}{\beta}\right)^2 - \upsilon^2\right\}}\right], \qquad F = \frac{Hk_\perp P_\perp}{\beta m_e}$$

$$H = \left\{\frac{(\beta m_e)^2}{P_\perp}\right\}\left(\frac{\partial f_0}{\partial P_\perp}\right)\left(\frac{P_z}{\beta m_e}\right) + \beta m_e\left(\frac{\partial f_0}{\partial P_z}\right), \qquad G = \frac{Hk_\perp \upsilon \Gamma_x}{\beta\left\{\left(\frac{\omega_c}{\beta}\right)^2 - \upsilon^2\right\}} \qquad ...(8)$$

$$J_n(\lambda_1) = \frac{dJ_n(\lambda_1)}{d\lambda_1} \text{ and } J_n(\lambda_2) = \frac{dJ_p(\lambda_2)}{d\lambda_2}$$

The Bessel function arguments are defined as

$$\lambda_1 = \frac{k_\perp P_\perp}{\omega_c m_e}\frac{k_\perp \Gamma_x}{\beta\left\{\left(\frac{\omega_c}{\beta}\right)^2 - \upsilon^2\right\}} \text{ and } \lambda_3 = \frac{k_\perp \upsilon \Gamma_x}{\beta\left\{\left(\frac{\omega_c}{\beta}\right)^2 - \upsilon^2\right\}}$$

The conductivity tensor ||σ|| is found to be

$$\|\sigma\| = \frac{-i\sum\left(e^2/\beta m_e\right)^2 \omega \int d^3 P J_g(\lambda_3)\| s \|}{\left[\omega - \left(\frac{k_\| P_z}{\beta m_e}\right) - \left((n+g)\frac{\omega_c}{\beta}\right) + pv\right]}$$

where

$$\| S \| = \begin{vmatrix} P_\perp J_n^2 J_p\left(\frac{n}{\lambda_1}\right)U^* & iP_\perp J_n V^* & P_\perp J_n^2 J_p\left(\frac{n}{\lambda_1}\right)W^* \\ P_\perp J_n J_n J_p\left(\frac{n}{\lambda_1}\right)U^* & iP_\perp J_n V^* & P_\perp J_n J_p\left(\frac{n}{\lambda_1}\right)W^* \\ P_z J_n^2 J_p\left(\frac{n}{\lambda_1}\right)U^* & iP_z J_n V^* & P_z J_n^2 J_p\left(\frac{n}{\lambda_1}\right)W^* \end{vmatrix}$$

By using these in the Maxwell's equations we get the dielectric tensor,

$$\varepsilon_{ij} = 1 + \sum\left\{\frac{4\pi e_s^2}{(\beta m_e)^2 \omega}\right\}\int \frac{d^3 P J g(\lambda_3)\| S \|}{\left(\omega - \frac{k \| Pz}{\beta m_e}\right) - \left\{\frac{(n+g)\omega_c}{\beta}\right\} + pv}$$

For parallel propagating whistler mode instability, the general dispersion relation reduces to $\varepsilon_{11} \pm E_{12} = N^2$ where

$$N^2 = \frac{k^2 c^2}{\omega^2}$$

The dispersion relation for relativistic case with perpendicular AC electric field for g= o, p = 1, n = 1 is written as:

$$\frac{k^2c^2}{\omega^2}=1+\frac{4\pi e_s^2}{(\beta m_e)^2\omega^2}\int\frac{d^3P}{\beta}\left[\frac{P_\perp}{2}-\frac{\upsilon\Gamma_x m_e}{2\left(\frac{\omega_c^2}{\beta^2}-\upsilon^2\right)}\right]\left[\left(\beta\omega-\frac{k_\parallel P_\parallel}{m_e}\right)^2\frac{\partial f_0}{\partial P_\perp}+\frac{P_\perp k_\parallel}{m_e}\frac{\partial f_0}{\partial P_\perp}\right]\frac{1}{\beta\omega-\frac{k_\parallel P_\parallel}{m_e}-\omega_c+\beta\upsilon} \quad ...(9)$$

The generalization distribution function (Dory et al. 1965; Sazhin et al. 1988) is given as

$$f_0=\left\{n_o P_\perp^{2j}/\pi^{3/2}P_{o\perp}^{2(j+1)}P_{o\perp}j!\right\}\exp\left[\left(-P_\perp/P_{o\perp}\right)^2-\left(P_\parallel/P_{o\parallel}\right)^2\right] \quad ...(10)$$

Where $P_{o\perp}$ and $P_{o\parallel}$ are perpendicular and parallel momenta for a temperature T. Substituting $4\pi e_s^2 n_o/m_e=\omega_p^2$ and integrating equation (9) by parts, the dispersion relation is found as

$$\frac{k^2c^2}{\omega^2}=1-\frac{\omega_p^2}{\omega^2}\int\frac{d^3P}{\beta}\left[1-\frac{\upsilon\Gamma_x m_e}{P_\perp\left(\frac{\omega_c^2}{\beta^2}-\upsilon^2\right)}\right]\left[\frac{\left(\beta\omega-\frac{k_\parallel P_\parallel}{m_e}\right)}{\left(\beta\omega-\frac{k_\parallel P_\parallel}{m_e}-\omega_c+\beta\upsilon\right)}-\frac{P_\perp^{\,2}}{2m_e^2c^2}\frac{\left(\omega^2-k_\parallel^2c^2\right)}{\left(\beta\omega-\frac{k_\parallel P_\parallel}{m_e}-\omega c+\beta\upsilon\right)^2}\right]f_o \quad ...(11)$$

When we remove AC field and set j=0 for bi-Maxwellian only, the relation becomes similar to (Chu et al. 1978)

$$\frac{k^2c^2}{\omega^2}=1-\frac{\omega_p^2}{\omega^2}\int\frac{d^3P}{\beta}\left[\frac{\left(\beta\omega-\frac{k_\parallel P_\parallel}{m_e}\right)}{\left(\beta\omega-\frac{k_\parallel P_\parallel}{m_e}-\omega_c\right)}-\frac{P_\perp^{\,2}}{2m_e^2c^2}\frac{\left(\omega^2-k_\parallel^2c^2\right)}{\left(\beta\omega-\frac{k_\parallel P_\parallel}{m_e}-\omega_c\right)^2}\right]f_o \quad ...(12)$$

Using equations (10) and (11) and doing some lengthy integrals the general dispersion relation becomes

$$\frac{k^2c^2}{\omega^2}=1+\frac{\omega_p^2}{\omega\beta^2P_{o\perp}^{2(j+1)}j!}\left[X_i\frac{\beta m_e\omega}{k_\parallel P_{0\parallel}}Z(\xi)+X_2(1+\xi Z(\xi))-X_5\frac{\omega^2}{k^2c^2}(1+\xi Z(\xi))\right]-\frac{\omega}{\omega\pm\omega_c}\frac{\omega_{pc}^2}{\omega_p^2\omega} \quad ...(13)$$

Where,

$$X_1=P_{o\perp}^{2(j+1)}-\frac{\upsilon\Gamma_x m_e}{\left(\frac{\omega_c}{\beta}\right)^2-\upsilon^2}(j-\frac{1}{2})!\,P_{o\perp}^{2j+1}$$

$$X_2=j!P_{o\perp}^{2(j+1)}\left(\frac{P_{o\perp}^2}{P_{o\parallel}^2}(j+1)-1\right)-\frac{\upsilon\Gamma_x m_e}{\left(\frac{\omega_c}{\beta}\right)^2-\upsilon^2}(j-\frac{1}{2})!P_{o\perp}^{2j+1}\times\left(\frac{P_{o\perp}^2}{P_{o\parallel}^2}(j+1)-1\right)$$

$$X_5 = \frac{P_{o\perp}^2}{P_{o\parallel}^2}\left[(j+1)!P_{o\perp}^{2(j+1)} - \frac{\upsilon\Gamma_x m_e}{\left(\frac{\omega_c}{\beta}\right)^2 - \upsilon^2}(j+\frac{1}{2})!P_{o\perp}^{2(j+1)}\right]$$

$$\xi = \frac{\beta m_e\omega - m_e\omega_c + \beta m_e\upsilon}{k_\parallel P_{o\parallel}}$$

For real k and substituting $k^2c^2/\omega^2 >> 1$, using an asymptotic expansion of $Z(\xi)$ in the limit of a large value of ξ, for $\omega = \omega_r + i\gamma$

The expression for growth rate for real frequency ω_r in dimensionless form is found to be

$$\frac{\gamma}{\omega_c} = \frac{\frac{\sqrt{\pi}}{\tilde{k}\beta}\left(\frac{X_2}{X_1} - k_3\right)k_4^3 \exp\left\{-\left(\frac{k_4}{k}\right)\right\}^2}{1+\beta X_4 + \frac{\tilde{k}^2}{2}\left(\frac{1+\beta X_4}{k_4^2} + \frac{2X_5\beta X_3 P_{o\parallel}^2}{X_1\tilde{k} - c^2}\right) - \frac{\tilde{k}^2}{k_4}\left(\frac{x_2}{x_1} - k_3\right) + \frac{(\delta-1)k_3^2}{(1+X_4)(1+X_3)^2}} \quad \ldots(14)$$

$$X_3 = \frac{k^2}{\delta\beta_1}\left[k_2(1+\beta X_4) + \frac{X_2}{X_1}\frac{\beta_1}{1+\beta X_4}\right]$$

Where $k_3 = \frac{\beta X_3}{k_4} + \frac{X_5}{X_1}\frac{\beta^2 X_3^2}{\tilde{k}^2}\frac{P_{o\parallel}^2}{c^2}$, $\tilde{k} = \frac{k_\parallel P_{o\parallel}}{m_e\omega_c}$

$$k_4 = 1 - \beta X_3 + \beta X_4, \quad X_3 = \frac{\omega_r\beta}{\omega_c}, \quad X_4 = \frac{\omega'}{m_e\omega_c}, \quad \omega' = m_e\beta\upsilon$$

$$\beta_1 = \frac{k_B T_\parallel \mu_0 n_0}{B_0^2}, \qquad \delta = 1 + \frac{n_c}{n_w}k_2(1+X_4) \quad \ldots(15)$$

Result and Discussion

To study the variation of dimensionless growth rate of whistler mode waves for relativistic and non-relativistic background plasma for various distribution index loss cone strength j=0 and j=1 with cold injection of electrons. Numerical calculations have been performed with reported ambient magnetic field of magnitude B_o=2.4x10^{-10}T and temperature anisotropy, A_T, varying between 0.25 and 0.75. The thermal energy ($K_BT_{\parallel}$) for relativistic and non-relativistic background plasma for j=0 and j=1 is 10eV, electron density for background plasma (n_w) is 5x10^4 m^{-3} for magnitude of AC electric field E_o= 4 mV/m and the values of AC frequency (υ) as 6 Hz, 12 Hz and 18 Hz. The relativistic factor v/c=0.3 is used. Now the cold injection electron density (n_c) is varied from 2.5x10^{5}m^{-3}, 5x10^{5}m^{-3} and 1.5x10^6 m^{-3}.

In **figure 1(a)** variation of relativistic growth rate with respect to $\tilde{k}$ for various values of AC frequency for j=0 is shown at A_T=0.25 and other parameters as mentioned in figure caption. The

growth rate for υ=6Hz is 0.0850 at $\tilde{k}$=0.95, the growth rate for υ=12 Hz is 0.0932 at $\tilde{k}$=1.05 and for υ=18Hz, the growth rate is γ/ω_c=0.1007 at $\tilde{k}$=1.15. This implies growth rate increases for higher AC frequencies and bandwidth shifts to higher values of $\tilde{k}$. As the growth rate is affected by dispersion function, the dispersion function is modified due to AC frequency in case of perpendicular electric field. Thus explaining increase in growth rate with increase in AC frequencies. In **figure 1(b)** variation of relativistic growth rate with respect to $\tilde{k}$ for various values of AC frequency for j=1 is shown where other parameters are as mentioned in figure caption. The growth rate for υ=6Hz is 0.8849 at $\tilde{k}$=0.89, the growth rate for υ=12 Hz is 1.0943 at $\tilde{k}$=1.0 and for υ=18Hz, the growth rate is γ/ω_c=1.2934 at $\tilde{k}$=1.15. This implies that growth rate increases for higher AC frequencies and bandwidth shifts to higher values of $\tilde{k}$. So in this case, we can conclude that frequency of AC field brings maxima to different wave number, just as resonant charged particles are oscillating at different cyclotron frequencies and thus gaining energy. In **figure 1(c)** variation of non-relativistic growth rate with respect to $\tilde{k}$ for various values of AC frequency for j=1 is shown where other parameters are as mentioned in figure caption. The growth rate for υ=6Hz is 0.8032 at $\tilde{k}$=0.85, the growth rate for υ=12 Hz is 0.9888 at $\tilde{k}$=1.0 and for υ=18Hz, the growth rate is γ/ω_c=1.1696 at $\tilde{k}$=1.1. This implies growth rate increases for higher AC frequencies and bandwidth shifts to higher values of $\tilde{k}$. The main factor contributing to cyclotron growth or the damping of waves is the energy exchange between the component of wave electric field, electrons and the AC field perpendicular to magnetic field.

Figure 2(a) shows variation of relativistic growth rate with respect to $\tilde{k}$ for various values of temperature anisotropy in background plasma for j=0 and other parameters as mentioned in figure caption. For A_T=0.25, growth rate is 0.1007 at $\tilde{k}$=1.15, for A_T=0.5, growth rate is 0.2527 at $\tilde{k}$=1.2 and for A_T=0.75, growth rate is 0.4374 at $\tilde{k}$=1.2. Hence growth rate increases with increasing value of temperature anisotropy. So it can be concluded that the major source of free energy is temperature anisotropy. **Figure 2(b)** shows variation of relativistic growth rate with respect to $\tilde{k}$ for various values of temperature anisotropy in background plasma for j=1 and other parameters as mentioned in figure caption. For A_T=0.25, growth rate is 1.2934 at $\tilde{k}$=1.15, for A_T=0.5, growth rate is 2.3051 at $\tilde{k}$=1.05 and for A_T=0.75, growth rate is 4.0757 at $\tilde{k}$=1.0. Since the growth rate increases significantly with increasing value of temperature anisotropy, it is inferred that the effect of temperature anisotropy is more prominent for loss-cone index j=1 than in case of relativistic background with j=0. **Figure 2(c)** shows variation of non- relativistic growth rate with respect to $\tilde{k}$ for various values of temperature anisotropy in background plasma with j=1 and other parameters as mentioned in figure caption. For A_T=0.25, growth rate is 1.1696 at $\tilde{k}$=1.1, for A_T=0.5, growth rate is 2.0139 at $\tilde{k}$=1.05 and for A_T=0.75, growth rate is 3.3594 at $\tilde{k}$=1.0. This implies that growth rate increases with increasing value of temperature anisotropy and bandwidth shifts to lower wave number region.

Using **figure 3(a)**, the variation of relativistic growth rate with respect to $\tilde{k}$ for various values of ratio of cold injected electron plasma to background plasma density (n_c/n_w) for j=0 is shown. The growth rate is 0.067 for n_c/n_w=5 at $\tilde{k}$=1.05, the growth rate is 0.1007 when n_c/n_w=10 at $\tilde{k}$=1.05 and growth rate is γ/ω_c=0.1201 for n_c/n_w =15 at $\tilde{k}$=1.25. This implies growth rate increases as number density of injected cold electrons increases. But the ratio of n_c/n_w increases as the radial distance increases, as reported by polar satellite (Laakdo et al. 2002). Using **figure 3(b)**, the variation of relativistic growth rate with respect to $\tilde{k}$ for various values of ratio of cold injected electron plasma to background plasma density (n_c/n_w) at j=1 is shown. The growth rate is 0.9175 for n_c/n_w=5 at $\tilde{k}$=0.95, the growth rate is 0.1301 when n_c/n_w=10 at $\tilde{k}$=1.25 and growth rate is γ/ω_c=2.0108 for n_c/n_w =15 at $\tilde{k}$=1.3. This implies as number density of injected cold electrons increases as the growth rate increases. Using **figure 3(c)**, the variation of non-relativistic growth rate with respect to $\tilde{k}$ for various values of ratio of cold injected electron plasma to background plasma density (n_c/n_w) at j=1 is shown. The growth rate is 0.6502 for n_c/n_w=5 at $\tilde{k}$=0.95, the growth rate is 1.1696 when n_c/n_w=10 at $\tilde{k}$=1.1 and growth rate is γ/ω_c=1.7921

for n_c/n_w =15 at $\tilde{k}$ =1.25. This shows Doppler shifting resonance conditions and increase in growth rate with increasing density of cold electron beam.

Figure 4(a) shows variation of relativistic growth rate with respect to $\tilde{k}$ for various values of relativistic factor v/c at j=0, other parameters being fixed and mentioned as figure caption. For v/c=0.3 and 0.6 the growth rate γ/ω_c is 0.1007 and 0.1297 respectively at $\tilde{k}$ =1.15. At v/c=0, growth rate is 0.0937 for same value of $\tilde{k}$ =1.15. As the velocity of energetic electrons increases growth rate also increases. **Figure 4(b)** shows variation of relativistic growth rate with respect to $\tilde{k}$ for various values of relativistic factor v/c at j=1, other parameters being fixed and mentioned as figure caption. For v/c=0.3, at $\tilde{k}$ =1.15 and 0.6 the growth rate γ/ω_c is 1.2934 and 1.9325 respectively. At v/c=0, growth rate is 1.1696 for same value of $\tilde{k}$ =1.1. This shows that increase in growth rate is more in case of relativistic background plasma than in case of non-relativistic background plasma. Also growth rate increases as the velocity of energetic electron increases.

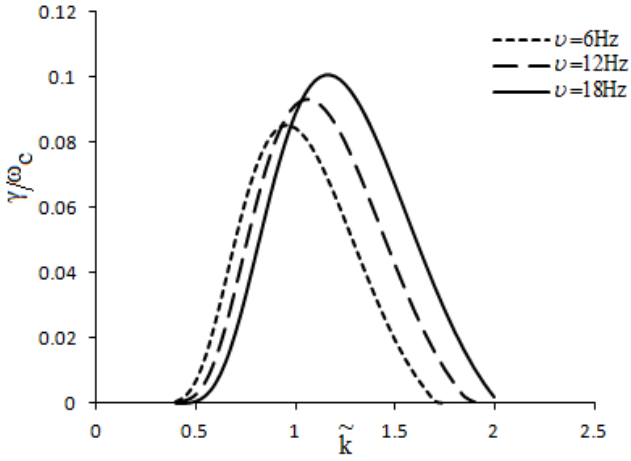

Figure 1(a): Variation of relativistic growth rate with $\tilde{k}$ for various values of AC frequencies having j=0, A_T=0.25, v/c=0.3 and n_c/n_w=10.

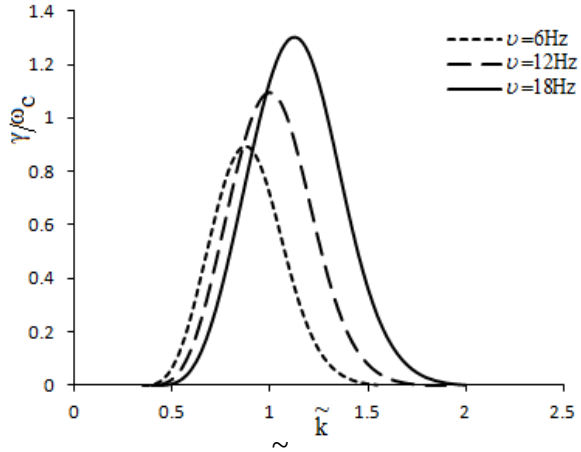

Figure 1(b): Variation of relativistic growth rate with $\tilde{k}$ for various values of AC frequencies having j=1, A_T=0.25, v/c=0.3 and n_c/n_w=10

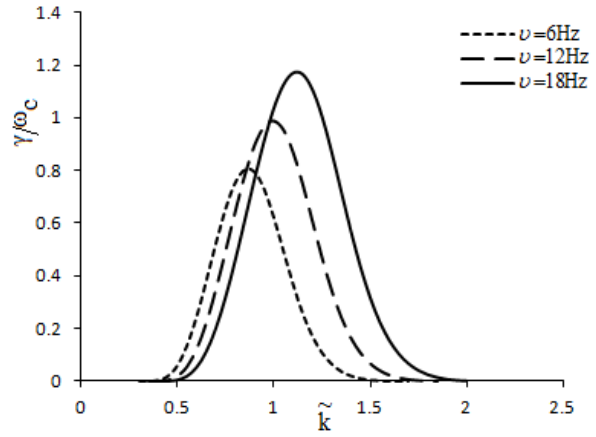

Figure 1(c): Variation of non-relativistic growth rate with $\tilde{k}$ for various values of AC frequencies having j=1, A_T=0.25 and n_c/n_w=10

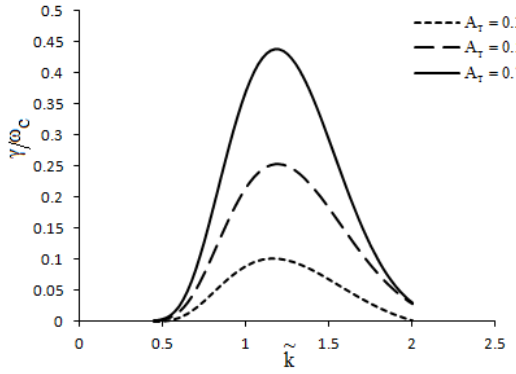

Figure 2(a): Variation of relativistic growth rate with $\tilde{k}$ for various values of temperature anisotropy having j=0, $\upsilon = 18\text{Hz}$, v/c=0.3 and n_c/n_w=10

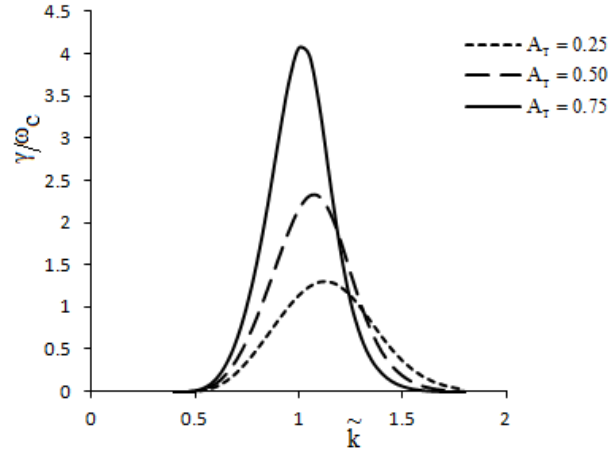

Figure 2(b): Variation of relativistic growth rate with $\tilde{k}$ for various values of temperature anisotropy having j=1, $\upsilon = 18\text{Hz}$, v/c=0.3 and n_c/n_w=10

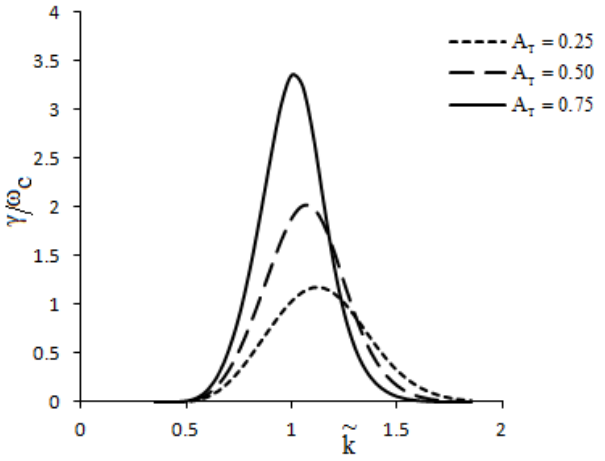

Figure 2(c): Variation of non-relativistic growth rate with $\tilde{k}$ for various values of temperature anisotropy having j=1, $\upsilon = 18\text{Hz}$, v/c=0.3 and n_c/n_w=10

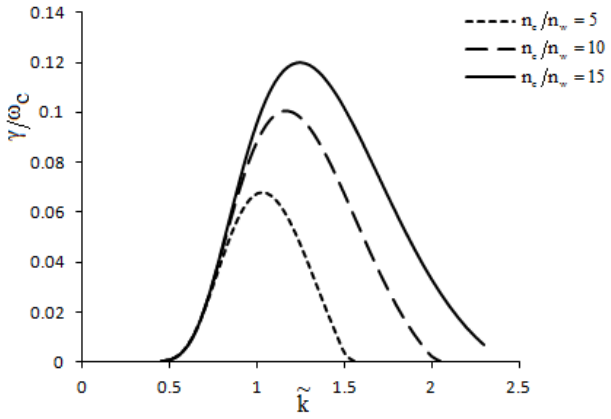

Figure 3(a): Variation of relativistic growth rate with $\tilde{k}$ for various values of ratio of number density of cold electrons to hot electrons having j=0, $\upsilon = 18\text{Hz}$, v/c=0.3 and A_T=0.25.

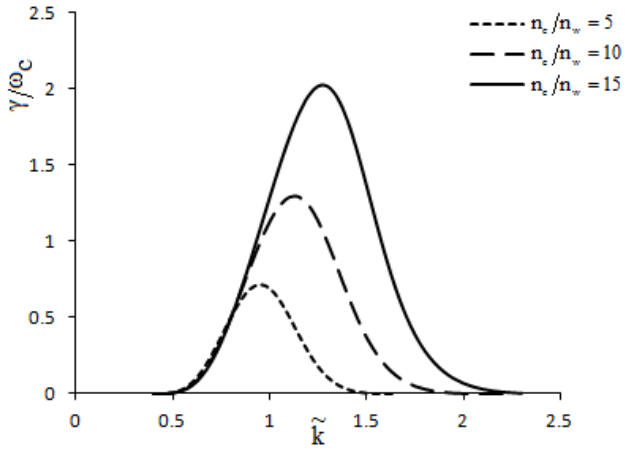

Figure 3(b): Variation of relativistic growth rate with $\tilde{k}$ for various values of ratio of number density of cold electrons to hot electrons having j=1, $\upsilon = 18\text{Hz}$, v/c=0.3 and A_T=0.25

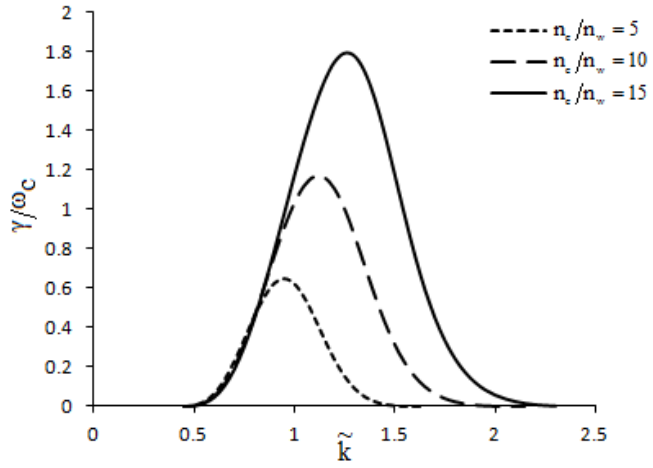

Figure 3(c): Variation of non-relativistic growth rate with $\tilde{k}$ for various values of ratio of number density of cold electrons to hot electrons having j=1, $\upsilon = 18\text{Hz}$ and A_T=0.25

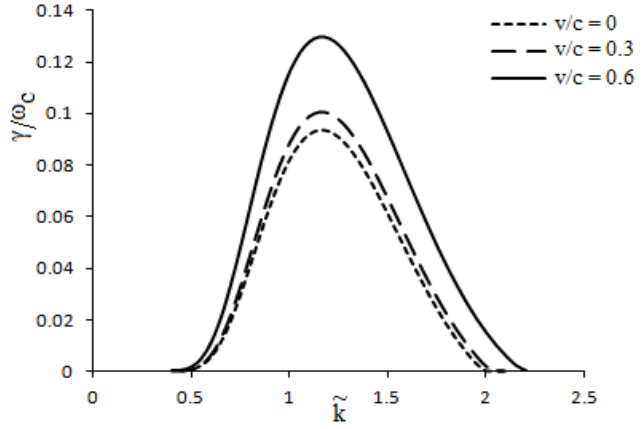

Figure 4(a): Variation of relativistic growth rate with $\tilde{k}$ for various values of relativistic factor having j=0, $\upsilon = 18\text{Hz}$, n_c/n_w=10 and A_T=0.25

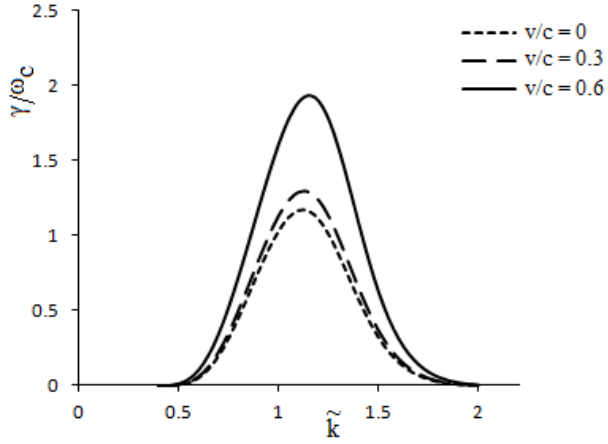

Figure 4(b): Variation of relativistic growth rate with $\tilde{k}$ for various values of relativistic factor having j=1, $\upsilon = 18\text{Hz}$, n_c/n_w=10 and A_T=0.25

References

Brice, N. M. and Lucas, C. (1971): Influence of Magnetospheric Convection and Polar Wind Loss of Electrons from the Outer Radiation Belts, J. Geophysical Res. 76: 90.

Chu, K. R., and Hirshfield, J. L. (1978): Comparitive Study of the Axial and Azimuthal Bunching Mechanism in Electromagnetic Cyclotron Instability, Phys. Fluid 21: 461.

Denton, R.E., Hudson, M.K. and Roth, I., (1992): Loss-cone Driven Ion Cyclotron Waves in the Magnetosphere, J. Geophysical Research 97: 12093.

Dory, R.A., Guest, G. E. and Harris, E. G. (1965): Unstable Electrostatic Plasma Waves Propagating Perpendicular to a Magnetic Field, Phys. Rev. Left. 14: 131.

Ganguli, G., Palmadesso, P. and Feeder, J. (1984): Temporal Evolution of Whistler Growth in a Cold Plasma Injection Experiment, J. Geophysical Rev. 89: 7351.

Gurnett, D. A. and Inan, U. S. (1988): Plasma Wave Observations with the Dynamics Explorer 1 spacecraft, Rev. Geophys. 26: 285.

Gurnett, D. A., Kurth, W.S. and Hospodersky, G. B. (2005): Radio and Plasma Waves Observations at Saturn from Cassini's Approach and First Orbit, Science 307*:* 1255.

Gurnett, D. A., Kurth, W.S. and Scarf, F. L. (1979b): Plasma Wave Observations near Jupiter: Initial Results from Voyager-2, Science 206: 987.

Gurnett, D. A., Kurth, W.S. and Roux, A., Bolten, S.J., Kennel, C.F (1996): Galileo Plasma Wave Observations in the Io Plasma Torus and Near Io, Science 274: 391.

Gurnett, D. A., Anderson, R. R., Scarf, F.L., Fedricks, R. W. and Smith, E. J. (1979a): Initial Results from the ISEE-1 and -2 Plasma Wave Investigation, Space Sci. Rev. 23: 103.

Gurnett, D. A., Kurth, W.S. and Poynter, R.L. (1989): First Plasma Waves Observations at Neptune, Science 246: 1494.

Gurnett D. A., Kurth W. S., Scarf F. L. and Poynter R. L. (1986): First Plasma Wave Observation at Uranus, Science 233: 106.

Huang, L., Hawkins, J.G. and Lee, L.C. (1990): On the Generation of Pulsating Aurora by the Loss-Cone Driven Whistler Instability in the Equatorial Region, J. Geophysical Research 95: 3893.

Kennel, C.F. and Petschek, H.E. (1966): Limits on Stably Trapped Particle Fluxes, Journal of Geophysical Research 71: 1-28.

Kurth, W. S., Barbosa, D. D., Gurnett, D. A. and Scarf, F.L. (1980): Electrostatic Waves in Jovian Magnetosphere, Geophys. Res. Letters 7: 57.

Kurth, W. S., Barbosa, D. D., Gurnett, D. A. and Scarf, F.L. (1987): Electrostatic Waves in the Magnetosphere of Uranus, Journal of Geophysical Research 92: 15225.

Kurth, W. S. and Gurnett, D. A. (1991): Plasma Waves in Planetary Magnetospheres, J. Geophys. Res. 96: 18977.

Kurth, W. S., Scarf, F. L, Gurnett, D. A. and Barbosa, D. D. (1983): A Survey of Electrostatic Waves in Saturns Magnetosphere, Journal of Geophysical Research 88: 8959.

Laakdo, H., Pfaff, R. and Janhunen, P. (2002): Polar Observations of Electron Density Distribution in the Earth's magnetosphere.2. Density Profiles, Ann. Geophys. 20: 1725.

Misra, K. D. and Pandey, R. S. (1995): Generation of Whistler Emissions by Injections of Hot Electrons in the Presence of a Perpendicular AC Electric Field, J. Geophys. Res. 100: 19405.

Misra, K. D., and Singh, B. D. (1980): On the Modification of Whistler Mode Instability in the Magnetosphere in the Presence of Parallel Electric Field by Cold Plasma Injection, J. Geophysical Res. 85: 5138.

Pandey, R. P., Karim, S. M., Singh, K.M, Misra, K.D. and Pandey, R. S, (2002): Current Driven Oblique Whistler Mode by Cold Plasma Injection in the Magnetosphere of Uranus, Indian J. Phys. 76B (5): 619.

Pandey, R. P., Karim, S. MD., Singh, K.M, Pandey, R. S. (2003): Effect of Cold Plasma Injection on Whistler Mode Instability Triggered by Perpendicular AC Electric Field at Uranus, Earth, Moon and Planets 91: 195.

Sazhin S. S. (1988): Oblique whistler Mode Growth and Damping in a Hot Anisotropic Plasma, Planet Space Science 36: 663.

Scarf, F. L., Gurnett, D. A. and Kurth, W. S. (1979): Jupiter Plasma Wave Observations: An Initial Voyager 1 overview, Science 204: 991.

Summers, D. and Thorn, R.M. (1995): Plasma Microinstabilities Driven by Loss-Cone Distribution, Journal of Plasma Physics 53: 293.

Zarka, P. (2004): Radio and Plasma Waves at the Outer Planets, Adv. Space Res. 33(11): 2045